Chemical Engineering Journal 147 (2009) 139–149

Contents lists available at ScienceDirect

Chemical Engineering Journal

journal homepage: www.elsevier.com/locate/cej

Adsorption of α-picoline onto rice husk ash and granular activated carbon from aqueous solution: Equilibrium and thermodynamic study

Dilip Hiradram Lataye [a], Indra Mani Mishra [b,*], Indra Deo Mall [b]

[a] Department of Civil Engineering, Visvesvaraya National Institute of Technology, Nagpur 440010, India
[b] Department of Chemical Engineering, Indian Institute of Technology Roorkee, Roorkee 247667, India

ARTICLE INFO

Article history:
Received 12 July 2007
Received in revised form 5 June 2008
Accepted 28 June 2008

Keywords:
α-Picoline
Rice husk ash (RHA)
Granular activated carbon (GAC)
Adsorption isotherms
Chi-square

ABSTRACT

In the present study, the batch adsorption experiments were carried out to calculate the adsorption capacities of rice husk ash (RHA) and commercial grade granular activated carbon (GAC) for the adsorption of α-picoline (Pi) from aqueous solutions. The effect of various parameters like initial pH (pH_0), adsorbent dose (m), contact time (t), initial concentration (C_0) and temperature (T) on the adsorption of Pi from the aqueous solutions was studied. The maximum uptake of Pi was observed to be 2.34 mg g^{-1} at lower concentration (50 mg dm^{-3}) and 15.46 mg g^{-1} at higher concentration (600 mg dm^{-3}) using 20 kg m^{-3} of RHA and the maximum uptake of Pi by GAC was observed to be 4.55 mg g^{-1} at lower concentration (50 mg dm^{-3}) and 36 mg g^{-1} at higher concentration (600 mg dm^{-3}) using 10 kg m^{-3} of GAC at normal temperature. The equilibrium data can be best represented by Radke–Prausnitz isotherm equation. However, Toth and Redlich–Peterson isotherm equations also represent the equilibrium data adequately. The values of change in Gibb's free energy (ΔG°), enthalpy (ΔH°) and entropy (ΔS°) were calculated. Thermodynamic study revealed that the adsorption of Pi onto RHA and GAC is an endothermic process. Isosteric heat of adsorption was found to be decreasing with an increase in surface loading. The acidic water and dilute acids showed higher desorption efficiency for Pi from RHA and GAC. Thus GAC can be regenerated by using acidic water and acids. However, RHA can be disposed off by using it as a fuel in furnaces to recover its energy value.

1. Introduction

α-Picoline (Pi), or 2-picoline, a derivative of pyridine, is a colourless liquid with nauseating odour and is used as a solvent, and as a raw material for various chemicals used in the manufacture of various polymers, textiles, fuels, agrochemicals, pharmaceuticals and colorants [1]. Pi is considered to be a hazardous chemical. Its properties are given in Table 1.

Various industrial units manufacturing pyridine and its derivatives, pharmaceutical units, etc. discharge Pi-bearing wastewaters. The typical concentration of Pi in wastewaters produced in a multidrug intermediates-product plant manufacturing pyridine and pyridine derivatives ranges from 20 to 200 mg dm^{-3}. The concentrations may exceed the range in case of emergency discharge and spill-episodes.

Various physico-chemical and biological treatment techniques are suggested for the treatment of Pi-bearing wastewaters, which include concentration followed by incineration [4], adsorption [5], biodegradation [6], etc. Adsorption can be used, provided that the adsorbents are cheap, easily available, and, if possible, regenerable, and that they have large surface area and high sorption capacity for Pi. Agri-solid wastes generally fulfill these requirements. They have high affinity towards organic compounds and, in most cases, desorption of solutes from spent agri-solids may not be feasible. In such cases, the spent agri-wastes can be filtered from the aqueous solution, dewatered, dried and used as a fuel in the furnaces/incinerators to chemically transform the adsorbates and the carbonaceous matter of the adsorbents into innocuous combustion products with energy recovery. Bagasse fly ash (BFA) and Rice husk ash (RHA are agri-waste materials and are available almost free of cost from the dust collection equipment attached to the flue gas line downstream of the furnaces which use bagasse or rice husk as the fuel. RHA has high adsorption efficiency for the removal of Cd, Ni, Zn, Pb, Hg, etc. and also various dyes and carbonaceous compounds present in wastewaters [7–9]. Lataye et al. have used RHA

* Corresponding author. Tel.: +91 1332 285715; fax: +91 1332 273560.
E-mail address: imishfch@iitr.ernet.in (I.M. Mishra).

1385-8947/$ – see front matter © 2008 Elsevier B.V. All rights reserved.
doi:10.1016/j.cej.2008.06.027

Nomenclature

a_R	R–P isotherm constant ($dm^3\ mg^{-1}$)
b	constant in Temkin equation ($J\ mol^{-1}$)
B_1	constant in Temkin equation ($dm^3\ g^{-1}$)
C_0	initial concentration of Pi ($mg\ dm^{-3}$)
C_e	equilibrium concentration of Pi ($mg\ dm^{-3}$)
C_r	residual concentration of Pi ($mg\ dm^{-3}$)
ΔG°	Gibbs free energy change ($kJ\ mol^{-1}$)
ΔH°	enthalpy change ($kJ\ mol^{-1}$)
$\Delta H_{st,0}$	isosteric heat of adsorption at zero surface coverage ($kJ\ kg^{-1}$)
k_{rp}	Radke–Prausnitz isotherm constant $((mg\ g^{-1})/(mg\ dm^{-3})^{1/P})$
K_{ad}	Equilibrium constant for adsorption ($dm^3 g^{-1}$)
K_F	Freundlich constant ($dm^3\ mg^{-1}$)
K_L	Langmuir constant ($dm^3\ mg^{-1}$)
K_R	Redlich–Peterson constant ($dm^3\ mg^{-1}$)
K_{RP}	Radke–Prausnitz isotherm constant ($dm^3\ mg^{-1}$)
K_T	constant in Temkin equation ($dm^3\ mg^{-1}$)
K_{Th}	Toth isotherm constant $((mg\ dm^{-3})^{Th})$
m	adsorbent dose (g)
n	heterogenity factor
P	Radke–Prausnitz isotherm constant
q	adsorptive uptake of α-picoline ($mg\ g^{-1}$)
q_e	adsorptive uptake of Pi at equilibrium ($mg\ g^{-1}$)
q_t	adsorptive uptake of Pi at any time t ($mg\ g^{-1}$)
$q_{e,calc}$	calculated q_e ($mg\ g^{-1}$)
$q_{e,exp}$	experimental q_e ($mg\ g^{-1}$)
q_m	monolayer adsorptive uptake ($mg\ g^{-1}$)
q_{Th}	monolayer adsorptive uptake ($mg\ g^{-1}$)
R	universal gas constant ($J\ mol^{-1}\ K^{-1}$)
ΔS°	entropy change ($kJ\ mol^{-1}\ K^{-1}$)
t	contact time (min)
T	temperature (K)
Th	Toth isotherm constant
V	volume (dm^3)
W	weight of adsorbent (g)

Greek letters

β	exponent in Redlich–Peterson equation
λ_{max}	wavelength (nm)

and granular activated carbon (GAC) for the adsorptive removal of pyridine [10]. Mohan et al. [11] have used activated carbons (ACs) manufactured from agri-waste materials for the sorptive removal of pyridine and picolines. In our previous paper [5], we have presented the use of BFA as an adsorbent for the removal of Pi from aqueous solutions. In the present paper, we report the sorption of Pi from aqueous solutions onto RHA and commercial-grade GAC in a batch process, and compare the results with that of BFA and ACs. The effect of initial pH of the solution ($2 \le pH_0 \le 12$), adsorbent dose ($2 \le m \le 60\ g\ dm^{-3}$), contact time ($0 \le t \le 3$ d), initial Pi concentration ($50 \le C_0 \le 600\ mg\ dm^{-3}$) and temperature ($283 \le T \le 323$ K) on the sorption of Pi onto RHA and GAC has been investigated. Equilibrium characteristics of the sorption process have been investigated and the experimental data have been fitted to various equilibrium isotherm equations viz. Langmuir, Freundlich, Temkin, Redlich–Peterson, Toth and Radke–Prausnitz equations. The thermodynamic aspects of Pi removal, viz. the effect of temperature on the sorption process has been studied and the isosteric heat of adsorption has been estimated. Desorption experiments have been carried out to determine the recovery of Pi and to check the stability of the Pi-loaded adsorbent.

Table 1
Properties of Pi [1–3]

S. no.	Property	α-Picoline
1	Synonyms	2-Picoline, α-methylpyridine
2	Chemical formula	C_6H_7N
3	Molecular weight	93.13
4	Physical properties	Colourless liquid, strong unpleasant odor
5	Boiling point	129 °C
6	Freezing point	−70 °C
7	Flash point	102 °C
8	Soluble in	Water, alcohol, ether
9	OSHA PEL	TWA 2 $mg\ dm^{-3}$ (8 h exposure)
10	ACGIH TLV	5 $mg\ dm^{-3}$ (STEL, 15 min)
11	Health effects	Poison by intraperitorial route, moderately toxic by ingestion, skin contact, intravenous and subcutaneous routes. Mildly toxic by inhalation, skin and severe eye irritant. Can cause CNS depression, gastrointestinal upset, and liver and kidney damage

2. Materials and methods

2.1. Adsorbent and its characterization

RHA, obtained from Bhawani Paper Mills, Raebareli, U.P. (India) was washed once with hot tap water (70 °C), dried and sieved using IS sieves (IS: 437, 1979). The sieved mass fraction between 180 and 600 μm was used for the sorption study. The GAC, obtained from Zeotec Adsorbents, New Delhi (India), in the sieved size range of 500–1700 μm was used for the sorption of Pi from its aqueous solutions. The physico-chemical characteristics of RHA and GAC were determined using standard methods [APHA, 1998]. Proximate analysis of both the adsorbents was carried out using standard procedure (IS: 1350, 1984, part-I). Bulk density was determined using a MAC bulk density meter. Scanning electron microscopy (SEM) micrographs of samples were obtained using a scanning electron microscope (LEO 435 VP). X-ray diffraction (XRD) analyses of the adsorbents were carried out using Phillips diffraction unit (Model PW 1140/90), with copper as the target and nickel as the filter media and K radiation maintained at 1.542 Å.

The specific surface area and the pore diameter of RHA and GAC particles were measured by nitrogen adsorption isotherm by using an ASAP 2010 Micromeritics instrument and by the Brunaer–Emmett–Teller (BET) method, using the software of Micromeritics. Nitrogen was used as cold bath (77.15 K). The Barrett–Joyner–Halenda (BJH) method was used to calculate the mesopore distribution.

2.2. Adsorbate

All the chemicals used in the study were of analytical reagent grade. The adsorbate, Pi (chemical formula = C_6H_7N, formula weight = 93.13) was supplied by Acros Organics (USA). An accurate volume of aqueous Pi solution was taken and mixed well with double-distilled water (DDW) to prepare a stock solution of 1000 $mg\ dm^{-3}$ Pi concentration. The stock solution was successively diluted with DWW to obtain the desired test concentration of Pi.

2.3. Analytical measurements

The stability of Pi in the concentration range of 50–600 $mg\ dm^{-3}$ in aqueous solution has been studied. No change in the Pi

concentration over a time period of 12 h was observed. No loss of Pi due to its vaporization has been observed during the experiments carried out in the stoppered/capped glass containers and also the analysis. A Perkin Elmer Lambda 35 double beam spectrophotometer was used to determine the concentrations of Pi in the aqueous solutions. The wavelength corresponding to maximum absorbance (λ_{max}) of Pi was found out by scanning a standard solution of known concentration at different wavelengths. The λ_{max} as determined from this plot was found to be 262 nm and this λ_{max} was used to prepare a calibration plot between absorbance and Pi concentration (mg dm^{-3}) in aqueous solution. The linear region of this curve was further used for the determination of Pi concentration of the unknown aqueous samples. Samples of higher concentrations of Pi beyond the linear region of the calibration curve were diluted with DDW, whenever necessary, for the accurate determination of its concentration from the linear portion of the calibration curve.

2.4. Batch adsorption study

All the batch experiments were carried out at 30 ± 1 °C. For each experimental run, 0.05 dm^3 of Pi solution of known C_0, pH_0 and m, taken in a 0.25 dm^3 stoppered conical flask, was agitated in a temperature-controlled orbital shaker at a constant speed of 150 ± 5 rpm. Samples were withdrawn at appropriate time intervals and centrifuged using a research centrifuge (Remi Instruments, Mumbai, India). The residual Pi concentration (C_r) of the centrifuged supernatant was then determined. Effect of pH_0 on Pi removal was studied over a range of $2 \le pH_0 \le 13$ by adjusting pH_0 with the help of 0.1 N H_2SO_4 and 0.1 N NaOH solutions. For the determination of the optimum m, a 0.05 dm^3 Pi solution was contacted with different amounts of adsorbents (m) till the equilibrium was attained. The effect of contact time up to 12 h on the Pi removal was also studied. For this purpose, 0.05 dm^3 solution with optimum m was kept for shaking in orbital shaker in several 0.25 dm^{-3} capacity conical flasks and the samples were withdrawn at appropriate time intervals. Equilibrium sorption studies were carried out by using Pi solutions ($50 \le C_0 \le 600$ mg dm^{-3}) with a known m and agitating them till equilibrium was attained. The effect of T ($283 \le T \le 323$ K) on equilibrium adsorption was also studied. Blank runs with only the adsorbent in 0.05 dm^3 of DDW were carried out simultaneously, at similar conditions, to account for any Pi leaching by the RHA and GAC, and any adsorption by glass containers. Similarly, blank runs with Pi solution (C_0 = 100 mg dm^{-3}) and without the adsorbents were also carried out. No change in the Pi concentration was observed over a time period of 12 h. The adsorption of Pi by the adsorbents at any time was calculated as follows:

$$q_t = \frac{(C_0 - C_t)V}{W} \quad (1)$$

where C_0 and C_t are Pi concentrations (mg dm^{-3}) in the solution at t = 0 and any t, V is the volume (dm^3), W is the weight (g) of the adsorbent and q_t is the adsorptive uptake of Pi by the adsorbent (mg g^{-1}) for any time t. At equilibrium, q_t and C_t are replaced by q_e and C_e, respectively.

3. Results and discussion

3.1. Characterization of adsorbent

The physico-chemical properties of RHA and GAC such as bulk density (mass per unit bed volume), BET surface area, moisture, volatile matter, ash and fixed carbon are given in Table 2. The average particle size of RHA and GAC used in the study were found to be 412 μm and 1271 μm, respectively.

Table 2
Characteristics of RHA and GAC

Parameters	RHA	GAC
Average particle size (μm)	412	1271
Bulk density (kg m^{-3})	175.3	506.7
Moisture content (%)	1.1	4.41
Volatile matter content (%)	7.36	3.32
Ash content (%)	80.58	51.90
Fixed carbon content (%)	10.96	40.37
Heating value (MJ kg^{-1})	21.76	20.06
BET surface area (m^2 g^{-1})	65.36	171.05
BJH adsorption surface area of pores (m^2 g^{-1})	52.35	131.98
BJH desorption surface area of pores (m^2 g^{-1})	26.62	94.33
Cumulative pore volume (cm^3 g^{-1})	0.039	0.123
BET pore diameter (Å)	34.66	31.03
BJH adsorption average pore diameter (Å)	43.27	37.30
BJH desorption average pore diameter (Å)	58.34	45.86

The BET pore surface area of RHA is found to be 65.36 m^2 g^{-1}, whereas the BJH adsorption/desorption surface area of pores is found to be 52.35/26.62 m^2 g^{-1}. The single point total pore volume of pores (<2529.5 Å) is 0.0567 cm^3 g^{-1}, whereas cumulative pore volume of pores (17 < d < 3000 Å) is 0.0386 cm^3 g^{-1}. The average pore diameter by BET method is found to be 34.66 Å, whereas the BJH adsorption/desorption average pore diameter is found to be 43.27 Å/58.34 Å. Micropores (d < 20 Å) account for 36.1% (18.9 m^2 g^{-1}) of the pore surface area and 15% (0.0084 cm^3 g^{-1}) of the pore volume, mesopores (20 Å < d < 500 Å) account for 63.5% (33.2 m^2 g^{-1}) of the pore surface area and 71% (0.04 cm^3 g^{-1}) of the pore volume and the macropores (d > 500 Å) account for only 0.4% (0.2 m^2 g^{-1}) of the pore surface area and 14% (0.0081 cm^3 g^{-1}) of the pore volume of RHA.

The BET surface area of GAC is found to be 171.05 m^2 g^{-1}, whereas BJH adsorption/desorption surface area of pores is found to be 131.98/94.33 m^2 g^{-1}. The single point total pore volume of pores (<3394.24 Å) is 0.133 cm^3 g^{-1}, whereas cumulative pore volume of pores (17 < d < 3000 Å) is 0.123 cm^3 g^{-1}. The average BET pore diameter is 31.028 Å, whereas the BJH adsorption/desorption average pore diameter is 37.30 Å/45.86 Å. The pore size analysis shows that 23.9% (31.6 m^2 g^{-1}) of the pore surface area and 12% (0.015 cm^3 g^{-1}) of the pore volume of GAC are covered by micropores. 75.8% (100.0 m^2 g^{-1}) of the pore surface area and 82% (0.101 cm^3 g^{-1}) of the pore volume are accounted for by mesopores. Only 0.3% (0.4 m^2 g^{-1}) of the pore surface area and 6% (0.007 cm^3 g^{-1}) of the pore volume are covered by the macropores. Therefore, the RHA and GAC can be taken as predominantly mesoporous materials.

The SEM micrographs of blank and Pi loaded RHA and GAC are shown in Fig. 1. From the SEM micrographs of the virgin and Pi loaded adsorbents the surface texture and porosity of RHA and GAC are seen to have been altered after the adsorption of Pi. XRD patterns for blank and Pi loaded RHA and GAC are shown in Fig. 2. The major components identified in blank RHA are cristoballite (SiO_2), margaritasite [$(Cs, K, H_3O)_2(UO_2)_2V_2O_8\cdot(H_2O)$] and macedonite ($PbTiO_3$). In blank GAC, the major components are moganite (SiO_2), akdalaite [$(Al_2O_3)_4\cdot H_2O$] and tamarugite [$NaAl(SO_4)_2\cdot 6H_2O$]. Major pyridine compounds in Pi loaded RHA and GAC are identified as pyridine 2,3-diacarboxylic acid or quinolinic acid ($C_7H_5NO_4$), pyridine 2,4-dicarboxylic acid hydrate ($C_7H_5NO_4\cdot H_2O$) and pyridine 2,5-diacarboxylic acid hydrate ($C_7H_5NO_4\cdot H_2O$). These compounds are shown in Fig. 2 as Py 2, 3-DA, Py 2,4-DA and Py 2,5-DA respectively. The other compounds were zinc–picoline ($C_{20}H_{28}N_6S_2Zn$) and pyridine picrate ($C_{12}H_8N_4O_7$) identified at 2θ = ~24.4° and 21°.

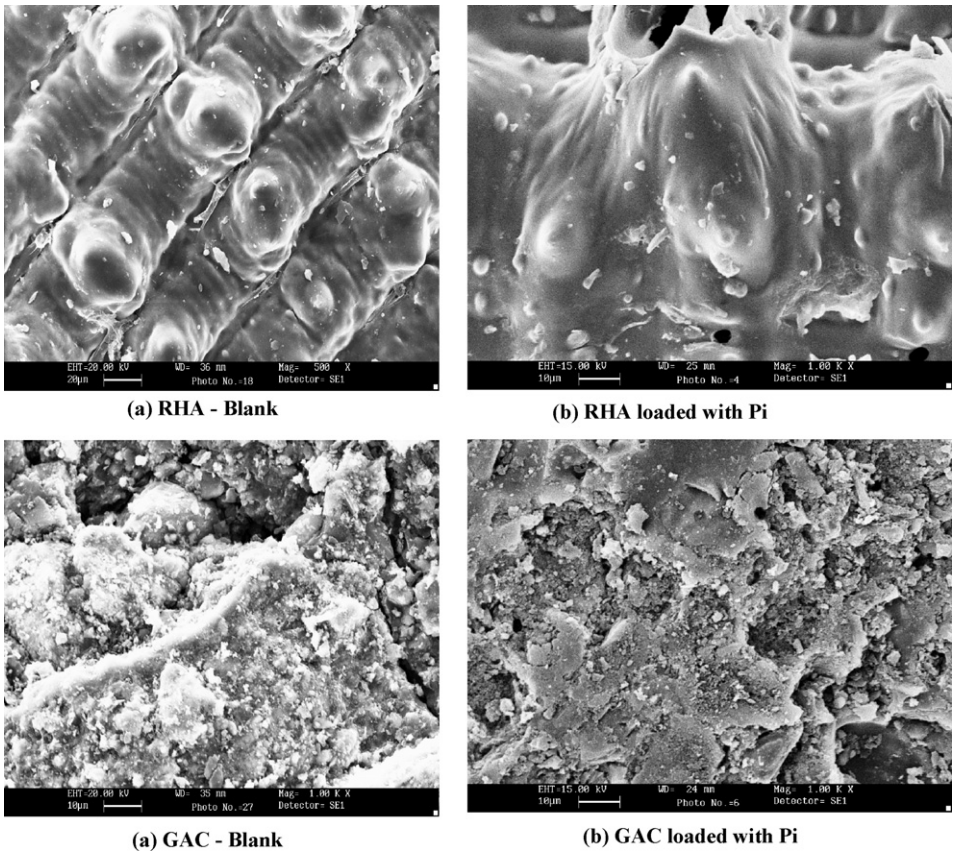

Fig. 1. SEM Micrographs of RHA and GAC at 1000×.

3.2. Effect of initial pH (pH_0) of the solution

Fig. 3 shows the effect of pH_0 on the Pi removal by RHA and GAC at $30 \pm 1\,^{\circ}C$, for $C_0 = 100\,mg\,dm^{-3}$ and $m = 20$ and $10\,g\,dm^{-3}$ after $t = 5\,h$ for RHA and GAC, respectively. A maximum Pi uptake of $\sim 4.5\,mg\,g^{-1}$ and $\sim 9.4\,mg\,g^{-1}$ was found to occur over $6 \leq pH_0 \leq 8$ by RHA and GAC, respectively. The maximum Pi removal of 92% and 94% was found to occur at the natural pH_0 ($pH_0 = 6.45$) of the aqueous Pi solution for RHA and GAC, respectively. The GAC has maximum surface area but shows only a marginal increase in efficiency over that of RHA. However, as the pH_0 decreases ($pH_0 < 4$), the adsorption efficiency also decreases.

Pi behaves like a base ($pK_a \sim 5.96$) [12], and the transition of Pi to PiH^+ is dependent on pH, with a maximum amount of PiH^+ occur-

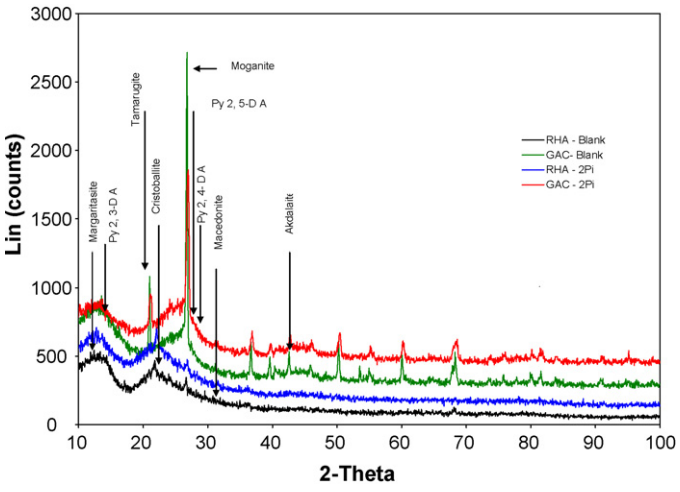

Fig. 2. XRD pattern of blank and Pi loaded RHA and GAC.

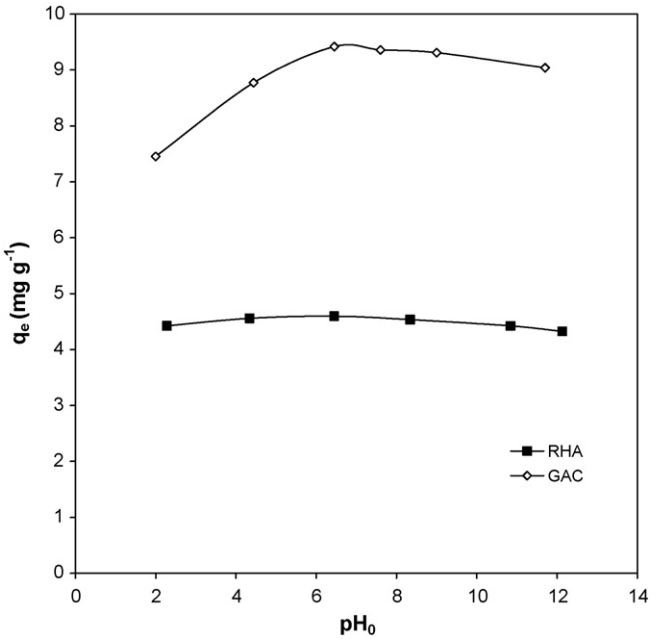

Fig. 3. Effect of initial pH_0 of the aqueous solution on the removal of Pi by RHA and GAC ($C_0 = 100\,mg\,dm^{-3}$, $m = 20\,g\,dm^{-3}$ for RHA and $10\,g\,dm^{-3}$ for GAC, $T = 303\,K$, $t = 5\,h$).

ring in the pH range of 4–10. The solution pH affects the surface charge of the adsorbents and, therefore, the adsorption proceeds through dissociation of functional groups, viz. surface oxygen complexes of acid character such as carboxyl and phenolic groups or of basic character such as pyrones or chromens, on the active sites of the adsorbent. pH can also affect the structural stability of Pi.

The chemical interaction of Pi with RHA or GAC (ADS) may be explained on the basis of the explanation put forth by Weber [13], Zhu et al. [14] and Lataye et al. [4,5,10]:

$$Pi + H^+ \rightleftharpoons PiH^+ \quad (a)$$

$$Pi + ADS \rightleftharpoons Pi\text{-}ADS \quad (b)$$

$$PiH^+ + M^+\text{-}ADS \rightleftharpoons PiH^+\text{-}ADS + M^+ \quad (c)$$

$$H^+ + PiH^+\text{-}ADS \rightleftharpoons H^+\text{-}ADS + PiH^+ \quad (d)$$

$$H^+ + ADS \rightleftharpoons H^+\text{-}ADS \quad (e)$$

$$Pi + H^+\text{-}ADS \rightleftharpoons PiH^+\text{-}ADS \quad (f)$$

Since Pi contains a nitrogen atom, which is more electronegative than an SP^2 hybridized C, Pi gets preferentially adsorbed on a positively charged surface [15]. At low pH ($pH_0 \leq 4$), the Pi gets converted to PiH^+ through protonation via Eq. (a) resulting in the low adsorption of protonated Pi on the positively charged ADS surface as shown by Eq. (c). At higher pH ($pH \geq 4$), π–π dispersion interactions also take place [16,17] and electrostatic interactions become important and Pi molecules are sorbed onto the adsorbents. The RHA and GAC have maximum affinity to Pi and PiH^+ for $6 \leq pH_0 \leq 8$. PiH^+ adsorption rate is lower than that of Pi molecules. Therefore, the dominant sorption reaction (at $pH_0 \approx 6.45$) is perhaps given by Eq. (b). Other reactions given by Eq. (a) and (c)–(f) play insignificant role in the overall sorption process of Pi onto RHA and GAC. Similar results were observed earlier for the adsorptive removal of pyridine and 2-picoline by bagasse fly ash [4,5].

3.3. Effect of adsorbent dose (m)

The effect of m on the uptake of Pi by RHA and GAC for $C_0 = 100\,mg\,dm^{-3}$ is shown in Fig. 4. The Pi removal increases rapidly with an increase in m up to $\sim 10\,g\,dm^{-3}$. The difference in Pi removal for $10 \leq m \leq 20\,g\,dm^{-3}$ of GAC is only marginal. At $m > 20\,g\,dm^{-3}$, the Pi removal remains almost unaffected. Therefore, $m = 10\,g\,dm^{-3}$ can be considered as the optimum dosage for GAC. Similarly, $m = 20\,g\,dm^{-3}$ can be considered as the optimum dosage for RHA. An increase in the Pi sorption with an increase in m can be attributed to the increase in the mesoporous surface area available for sorption, and hence, the availability of more adsorption sites. However, the unit adsorption decreases with an increase in m. The decrease in sorption capacity per unit weight of adsorbent is because of the fact that an increase in the sorbent dose at constant concentration and volume leads to the saturation of sorption sites through the sorption process [4,5,18,19]. Also, particle–particle interaction such as aggregation at higher m [4,5,20] leads to a decrease in the availability of total surface area of the sorbent and an increase in the diffusional path length [4,5,18]. Thus at

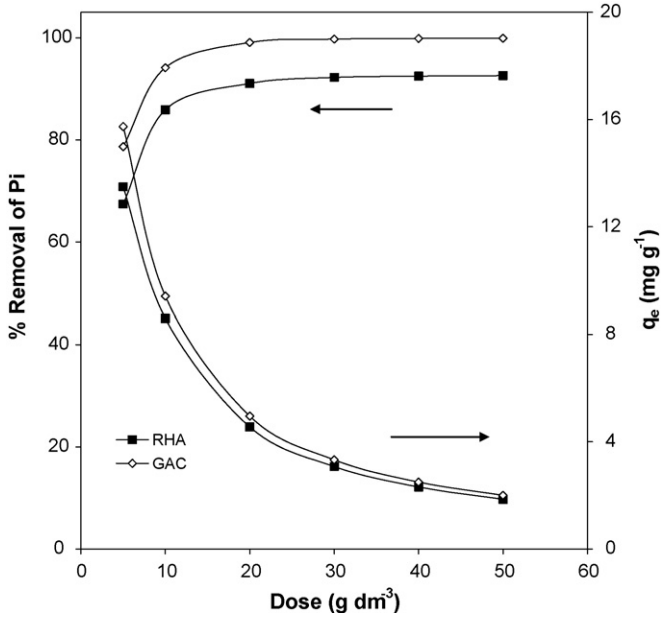

Fig. 4. Effect of m on the removal of Pi by RHA and GAC ($C_0 = 100\,mg\,dm^{-3}$, $pH_0 = 6.45$, $T = 303\,K$, $t = 5\,h$).

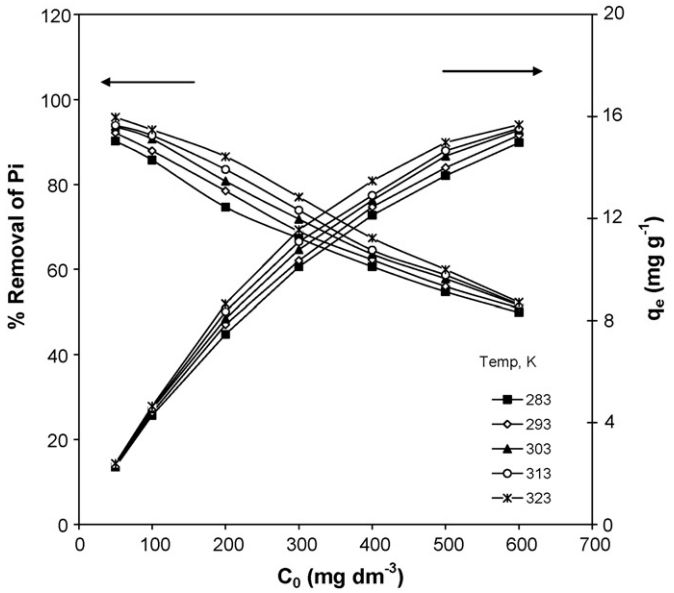

Fig. 5. Effect of C_0 and temperature on % removal and uptake of Pi by RHA ($m = 20\,g\,dm^{-3}$, $pH_0 = 6.45$, $t = 5\,h$).

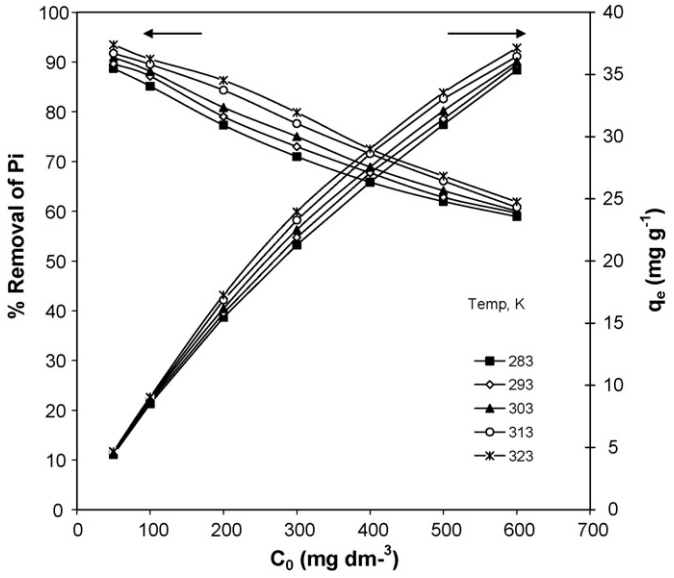

Fig. 6. Effect of C_0 and temperature on % removal and uptake of Pi by GAC ($m = 10\,g\,dm^{-3}$, $pH_0 = 6.45$, $t = 5\,h$).

Table 3
Isotherm parameters and Chi-square values for the adsorption of Pi onto RHA

Isotherms	Constants	Temperatures (K)				
		283	293	303	313	323
Langmuir, $q_e = \frac{q_m K_L C_e}{1+K_L C_e}$	K_L ($dm^3\ mg^{-1}$)	0.020	0.024	0.030	0.035	0.046
	q_m ($mg\ g^{-1}$)	16.807	16.750	16.694	16.639	16.584
	R^2 (linear)	0.985	0.987	0.990	0.993	0.996
	R^2 (non-linear)	0.993	0.994	0.995	0.997	0.998
	χ^2 (Chi-square)	0.734	0.857	1.021	0.716	0.837
Freundlich, $q_e = K_F C_e^{1/n}$	K_F ($dm^3\ mg^{-1}$)	1.193	1.404	1.649	1.758	2.092
	n	2.197	2.312	2.438	2.473	2.631
	R^2 (linear)	0.992	0.990	0.985	0.975	0.972
	R^2 (non-linear)	0.996	0.995	0.992	0.987	0.986
	χ^2 (Chi-square)	0.159	0.224	0.308	0.558	0.748
Temkin, $q_e = \frac{RT}{b} \ln(K_T C_e)$	B	3.112	3.026	2.939	2.939	2.817
	K_T ($dm^3\ mg^{-1}$)	0.314	0.409	0.546	0.613	0.902
	R^2 (linear)	0.975	0.980	0.986	0.994	0.994
	R^2 (non-linear)	0.987	0.990	0.993	0.997	0.997
	χ^2 (Chi-square)	0.908	0.732	0.471	0.223	0.294
Redlich–Peterson, $q_e = \frac{K_R C_e}{1+a_R C_e^{\beta}}$	a_R ($dm^3\ mg^{-1}$)	0.353	0.366	0.318	0.378	0.412
	K_R ($dm^3\ mg^{-1}$)	0.949	1.155	1.300	1.489	1.967
	β	0.688	0.714	0.758	0.745	0.778
	R^2 (linear)	1.000	1.000	1.000	0.999	0.999
	R^2 (non-linear)	1.000	1.000	1.000	0.999	1.000
	χ^2 (Chi-square)	0.010	0.003	0.219	0.047	0.054
Toth, $q_e = \frac{q_{Th} C_e}{\left[(1/K_{Th})+C_e^{Th}\right]^{1/Th}}$	Th	0.278	0.302	0.330	0.338	0.348
	q_{Th} ($mg\ g^{-1}$)	60.345	46.141	36.563	34.548	30.456
	K_{Th} ($mg\ l^{-1})^{Th}$	0.433	0.451	0.468	0.485	0.556
	R^2 (linear)	1.000	1.000	1.000	0.999	1.000
	R^2 (non-linear)	1.000	1.000	1.000	1.000	1.000
	χ^2 (Chi-square)	0.010	0.005	0.016	0.037	0.035
Radke–Prausnitz	P	0.700	0.722	0.754	0.800	0.851
	k_{rp} ($mg\ g^{-1}$)/($mg\ dm^{-3})^{1/P}$	2.884	3.307	4.024	5.249	7.052
	K_{RP} ($dm^3\ g^{-1}$)	0.301	0.330	0.320	0.231	0.197
	R^2 (linear)	1.000	1.000	1.000	1.000	1.000
	R^2 (non-linear)	1.000	1.000	1.000	1.000	1.000
	χ^2 (Chi-square)	0.012	0.003	0.011	0.009	0.051

$m > 10\ g\ dm^{-3}$ for GAC and $m > 20\ g\ dm^{-3}$ for RHA, the incremental Pi uptake is very small, as the surface concentration and the bulk solution concentration of Pi come to equilibrium to each other [21]. Thus, the optimum m for RHA and GAC can be taken as 20 and $10\ g\ dm^{-3}$, respectively.

3.4. Effect of initial concentration (C_0) and temperature

The equilibrium uptake of Pi by the adsorbents is affected by C_0 and T. Figs. 5 and 6 show the effect of C_0 ($50 \le C_0 \le 600\ mg\ dm^{-3}$) and T ($283 \le T \le 323$ K) on the equilibrium Pi uptake by RHA and GAC at their optimum m values, respectively. It is found that the Pi sorption increases with an increase in C_0 and T. The increase in q_e, with C_0 is attributed to the increase in the mass transfer driving force on account of an increase in C_0. Pi removal by RHA is ~52% and by GAC is ~60% at the highest $C_0 = 600\ mg\ dm^{-3}$ at 303 K. It should be noted that the Pi loading onto RHA and GAC increases with an increase in T. The increase in adsorption capacity is probably because of the creation of some new active sites on the surface of adsorbents [22]. The increase in the adsorption capacity of the adsorbents with an increase in T indicates that the sorption is an endothermic process.

3.5. Effect of contact time

The effect of contact time on the removal of Pi by GAC and RHA for $m = 10$ and $20\ g\ dm^{-3}$, respectively, for $C_0 = 100\ mg\ dm^{-3}$ is shown in Fig. 7. This figure shows rapid adsorption of Pi initially up to 15 min: >75% Pi sorption takes place with RHA and ~60% with GAC in the first 15 min. Thereafter, the Pi removal is very sluggish and the residual Pi concentration (C_r) in the solution is found to be

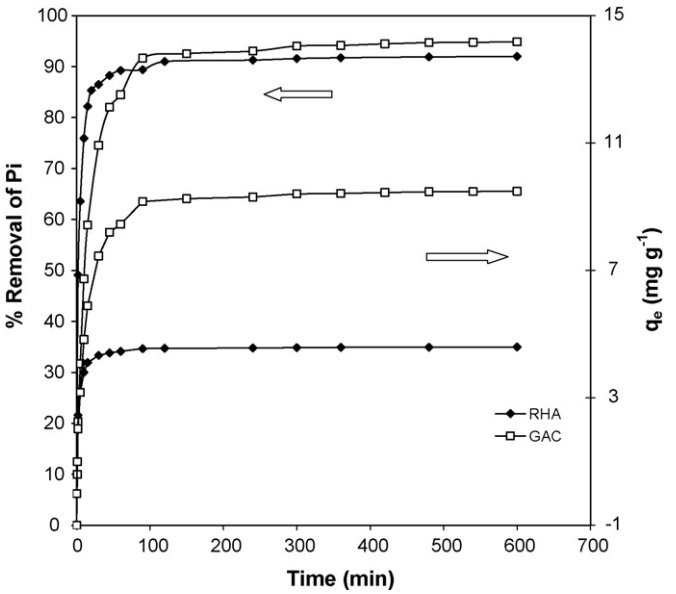

Fig. 7. Effect of contact time on the % removal and uptake of Pi by GAC and RHA at various C_0 values ($m = 20$ and $10\ g\ dm^{-3}$ for RHA & GAC res., $pH_0 = 6.45$, $T = 303$ K).

Table 4
Isotherm parameters and Chi-square values for the adsorption of Pi onto GAC

Isotherms	Constants	Temperatures (K)				
		283	293	303	313	323
Langmuir, $q_e = \frac{q_m K_L C_e}{1+K_L C_e}$	K_L ($dm^3\ mg^{-1}$)	0.015	0.017	0.021	0.023	0.027
	q_m ($mg\ g^{-1}$)	42.553	42.194	42.017	41.841	41.667
	R^2 (linear)	0.970	0.977	0.983	0.992	0.991
	R^2 (non-linear)	0.985	0.988	0.991	0.996	0.995
	χ^2 (Chi-square)	1.251	1.187	1.310	0.664	0.889
Freundlich, $q_e = K_F C_e^{1/n}$	K_F (($mg\ g^{-1}$) ($mg\ dm^{-3}$)$^{-1/n}$)	1.875	2.085	2.313	2.572	2.983
	n	1.855	1.899	1.948	1.977	2.067
	R^2 (linear)	0.996	0.992	0.991	0.982	0.982
	R^2 (non-linear)	0.998	0.996	0.996	0.991	0.991
	χ^2 (Chi-square)	0.161	0.331	1.288	1.101	1.237
Temkin, $q_e = \frac{RT}{b} \ln(K_T C_e)$	B	8.021	7.990	7.902	7.687	7.771
	K_T ($dm^3\ mg^{-1}$)	0.219	0.249	0.287	0.351	0.414
	R^2 (linear)	0.955	0.964	0.970	0.983	0.983
	R^2 (non-linear)	0.977	0.982	0.985	0.992	0.991
	χ^2 (Chi-square)	5.698	3.909	3.731	1.613	2.815
Redlich–Peterson, $q_e = \frac{K_R C_e}{1+a_R C_e^{\beta}}$	a_R ($dm^3\ mg^{-1}$)	0.336	0.274	0.231	0.200	0.239
	K_R ($dm^3\ mg^{-1}$)	1.566	1.590	1.665	1.752	2.226
	β	0.618	0.653	0.691	0.717	0.729
	R^2 (linear)	1.000	0.999	0.999	0.999	0.999
	R^2 (non-linear)	1.000	0.999	1.000	0.999	0.999
	χ^2 (Chi-square)	0.023	0.035	0.013	0.046	0.063
Toth, $q_e = \frac{q_{Th} C_e}{[(1/K_{Th})+C_e^{Th}]^{1/Th}}$	Th	0.231	0.305	0.336	0.371	0.405
	q_{Th} ($mg\ g^{-1}$)	406.643	172.422	131.181	105.394	84.628
	K_{Th} ($mg\ l^{-1}$)Th	0.368	0.300	0.291	0.278	0.280
	R^2 (linear)	0.999	0.999	0.999	0.999	0.999
	R^2 (non-linear)	1.000	0.999	1.000	0.999	1.000
	χ^2 (Chi-square)	0.026	0.050	0.018	0.056	0.054
Radke–Prausnitz, $q_e = \frac{K_{RP} k_{rp} C_e}{1+K_{RP} C_e^{P}}$	P	0.570	0.623	0.669	0.765	0.761
	k_{rp} ($mg\ g^{-1}$)/($mg\ dm^{-3}$)$^{1/P}$	3.532	4.873	6.382	11.211	11.001
	K_{RP} ($dm^3\ g^{-1}$)	0.601	0.383	0.284	0.141	0.185
	R^2 (linear)	1.000	1.000	1.000	1.000	1.000
	R^2 (non-linear)	1.000	1.000	1.000	1.000	1.000
	χ^2 (Chi-square)	0.015	0.032	0.008	0.004	0.038

~10% and ~15% after 1 h, ~8% and ~6% after 5 h, ~8% and ~5% after 12 h, ~7.8% and 4.7% after 24 h and ~7.4% and 4.5% after 72 h contact time for RHA and GAC, respectively. The initial sorption rate is rapid because of the availability of more adsorption sites. As there is not much difference in the C_r at $t = 5$ h, and 12 h, the steady-state sorption is assumed after 5 h and further experiments were carried out at $t = 5$ h only. The adsorptive uptake of Pi by GAC and RHA is very fast when compared to the adsorption rate of Pi onto activated carbons derived from coconut fibres and shells, with and without acid treatment, as reported by Mohan et al. [11]. This, despite the fact, that these ACs have higher surface area of 378 $m^2\ g^{-1}$ (activated carbon derived from coconut shells without any treatment, SAC) and 380 $m^2\ g^{-1}$ (activated carbon derived from acid-treated coconut shells, ATSAC).

3.6. Adsorption equilibrium

Three two-parameter isotherm equations, namely, Langmuir [23], Freundlich [24], Temkin [25]; and three three-parameter isotherm equations namely, Redlich–Peterson [26], Toth [27] and Radke–Prausnitz [28] have been used to fit the experimental data through linear and non-linear regression techniques to check for their adequacy to represent the experimental data. These isotherm equations (Tables 3 and 4) are well known and have been used by several authors including the present group [4,5,7,21].

The Langmuir [23] equation is given as

$$\frac{C_e}{q_e} = \frac{C_e}{q_m} + \frac{1}{K_L q_m} \tag{2}$$

where q_m is the mono-layer adsorption capacity ($mg\ g^{-1}$) and K_L is the Langmuir isotherm constant related to free energy of adsorption ($dm^3\ mg^{-1}$). The Freundlich [24] equation is given as

$$\ln q_e = \ln K_F + \left(\frac{1}{n}\right) \ln C_e \tag{3}$$

where K_F is a constant which indicates the sorption capacity of the adsorbent (($mg\ g^{-1}$) ($mg\ dm^{-3}$)$^{-1/n}$) and $1/n$ is a constant which gives the intensity of adsorption.

The Temkin isotherm [25] is given as

$$q_e = B_1 \ln K_T + B_1 \ln C_e \tag{4}$$

where $B_1 = RT/b$ is a constant related to heat of adsorption and b shows the variation of the adsorption energy ($J\ mol^{-1}$). K_T is a Temkin constant which takes into account the interactions between the adsorbate and the adsorbent ($dm^3\ mg^{-1}$).

Redlich–Peterson isotherm equations [26] is given as

$$q_e = \frac{K_R C_e}{1 + a_R C_e^{\beta}} \quad \text{or} \quad \ln\left(K_R \frac{C_e}{q_e} - 1\right) = \ln a_R + \beta \ln C_e \tag{5}$$

where K_R ($dm^3\ g^{-1}$) and a_R ($dm^3\ mg^{-1}$) are Redlich–Peterson isotherm constants and β is an exponent, the value of which lies between 0 and 1. For $\beta = 1$, Eq. (5) reduces to Langmuir equation, with $a_R = K_L$. At high adsorbate concentrations, Eq. (5) is transformed into Freundlich isotherm equation with $K_F = K_R/a_R$ and $1/n = 1 - \beta$.

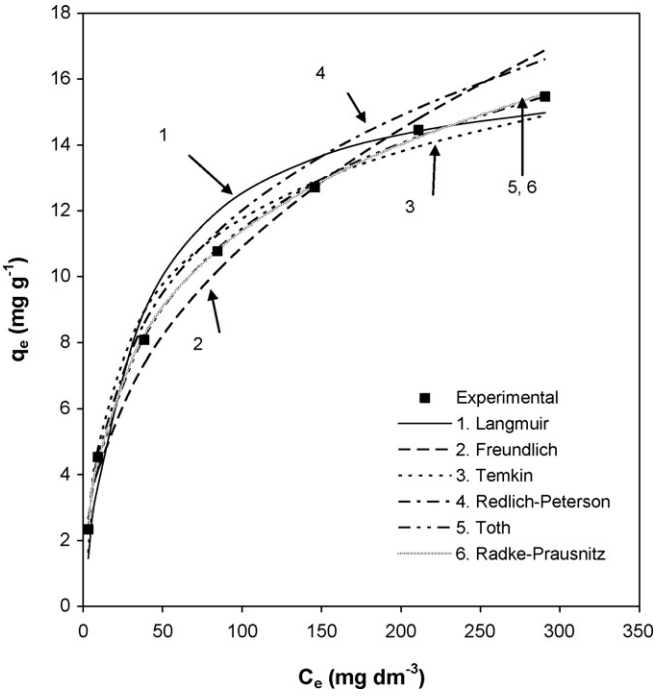

Fig. 8. Comparison of the fit of the various isotherm equations with the experimental sorption data for Pi onto RHA (T = 303 K, m = 20 g dm^{-3}, pH$_0$ = 6.45, t = 5 h).

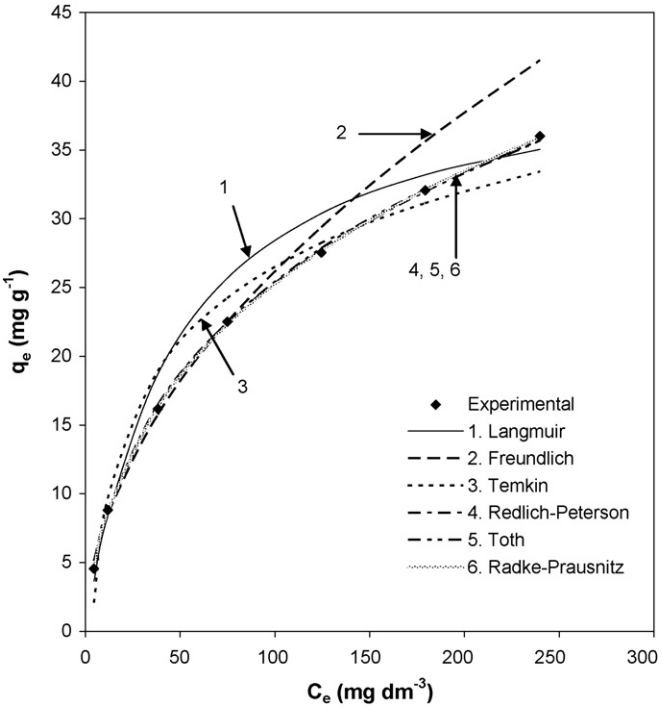

Fig. 9. Comparison of the fit of the various isotherm equations with the experimental sorption data for Pi onto GAC (T = 303 K, m = 10 g dm^{-3}, pH$_0$ = 6.45, t = 5 h).

Toth equation [27] is given as

$$q_e = \frac{q_{Th} C_e}{[(1/K_{Th}) + C_e^{Th}]^{1/Th}} \quad \text{or} \quad \left[\frac{C_e}{q_e}\right] = \frac{1}{(q_{Th})^{Th} K_{Th}} + \frac{C_e}{(q_{Th})^{Th}} \tag{6}$$

where q_{Th} is the monolayer adsorptive uptake (mg g^{-1}), K_{Th} is the Toth isotherm constant (mg dm^{-3})Th, and Th is the dimensionless Toth isotherm exponent which characterizes the heterogeneity of the system and is usually less than unity. The more Th deviates from unity, the larger is the heterogeneity of the adsorbent. When Th = 1, the Toth isotherm Eq. (6) reduces to Langmuir Eq. (2).

Radke–Prausnitz isotherm equation [28] is given as

$$q_e = \frac{K_{RP} k_{rp} C_e}{1 + K_{RP} C_e^P} \quad \text{or} \quad \frac{C_e}{q_e} = \frac{1}{K_{RP} k_{rp}} + \frac{C_e^P}{k_{rp}} \tag{7}$$

where K_{RP} (dm^3 g^{-1}) and k_{rp} [(mg g^{-1})/(mg dm^{-3})$^{1/P}$] are Radke–Prausnitz constants and P is a dimensionless exponent. For P = 1, Eq. (7) reduces to the Langmuir Eq. (2).

The isotherm parameters were determined by using the solver add-in function of the MS excel, for the fitting of the experimental data. The linear coefficient of determination and a non-linear Chi-square test have been used for the purpose. The Chi-square test is the sum of the squares of the differences between the experimental data and calculated data by using isotherm equations, with the square difference divided by the corresponding data calculated from the models. The Chi-square error analysis is given by

$$\chi^2 = \sum \frac{(q_{e,exp} - q_{e,calc})^2}{q_{e,calc}} \tag{8}$$

where $q_{e,exp}$ is the experimental equilibrium adsorption capacity (mg g^{-1}) and $q_{e,calc}$ is the adsorption capacity calculated by using the model equation.

The estimated values of the isotherm parameters, regression coefficients and Chi-square error functions are presented in Tables 3 and 4. Figs. 8 and 9 show the comparative fit of the predicted values from all the equilibrium isotherm equations with the experimental data. By comparing the results for the Chi-square values and the correlation coefficients for the isotherms for a particular adsorbent (Tables 3 and 4), it is found that the Pi adsorption onto RHA and GAC can be best represented by Radke–Prausnitz isotherm. However, Toth and Redlich–Peterson isotherms also give comparative fit and can also be used.

3.7. Estimation of thermodynamic parameters

The Gibbs free energy change (ΔG°) of the adsorption process is related to the adsorption equilibrium constant (K_{ad}) by the classical Van't Hoff equation [29]:

$$\Delta G^\circ = -RT \ln K_{ad} \tag{9}$$

It is also related to the change in entropy, ΔS° and the heat of adsorption, ΔH° at a constant temperature as follows:

$$\Delta G^\circ = \Delta H^\circ - T\,\Delta S^\circ \tag{10}$$

From the two equations, one gets,

$$\ln K = \frac{-\Delta G^\circ}{RT} = \frac{\Delta S^\circ}{R} - \frac{\Delta H^\circ}{R}\frac{1}{T} \tag{11}$$

where ΔG° is the free energy change (kJ mol^{-1}), ΔH° is the change in enthalpy (kJ mol^{-1}), ΔS° is the entropy change (kJ mol^{-1} K^{-1}), T is the absolute temperature (K) and R is the universal gas constant (8.314 J mol^{-1} K^{-1}). Thus, ΔH° can be determined by the slope of the linear Van't Hoff plot i.e. $\ln K_{ad}$ versus $(1/T)$, using the equation:

$$\Delta H^\circ = \left[R\frac{\mathrm{d}\ln K_{ad}}{\mathrm{d}(1/T)}\right] \tag{12}$$

This ΔH° corresponds to the isosteric heat of adsorption ($\Delta H_{st,0}$) with zero surface coverage (i.e. q_e = 0) [30]. K_{ad}, at q_e = 0 was obtained from the intercept of the $\ln(q_e/C_e)$ versus q_e plot [31,32]. Fig. 10 shows the Van't Hoff's plot from which the values of ΔH°, ΔS° and ΔG° for RHA and GAC have been calculated (Table 5).

It is observed from Table 5 that ΔH° and ΔS° have positive values, and ΔG° has negative values. The positive ΔH° value

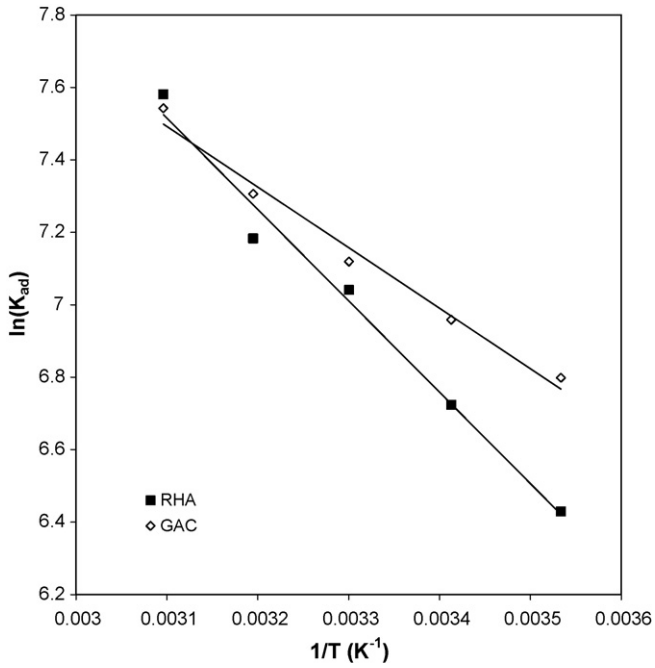

Fig. 10. Vant's Hoff plot for the determination of ΔH°, ΔS° and ΔG°.

confirms the endothermic nature of the overall-sorption process. The positive value of ΔS° suggests increased randomness at the solid/solution interface with some structural changes in the adsorbate and adsorbent and Pi affinity to the RHA and GAC. Therefore, the positive ΔS° value corresponds to an increase in the degree of freedom of the adsorbed species. The negative values of ΔG° indicate the feasibility and spontaneity of the adsorption process.

3.7.1. Isosteric heat of adsorption

Apparent isosteric heat of adsorption ($\Delta H_{st,a}$) at constant surface coverage, q_e (3–15 mg g^{-1} for RHA and 6–30 mg g^{-1} for GAC) was calculated using the Clausius–Clapeyron equation [32,33]:

$$\frac{d \ln C_e}{dT} = \frac{-\Delta H_{st,a}}{RT^2} \quad (13)$$

$$\Delta H_{st,a} = \left.\frac{d \ln C_e}{d(1/T)}\right|_{q_e} \quad (14)$$

C_e at constant q_e is obtained from the adsorption isotherm constants at different temperatures. $\Delta H_{st,a}$ is calculated from the slope of the ln(C_e) versus ($1/T$) plot (Figs. 11 and 12). $\Delta H_{st,a}$ for Pi sorption calculated from the figure are: 193.39, 179.14, 153.75, 117.29 and 66.75 kJ kg^{-1} for RHA at q_e = 3, 6, 9, 12 and 15 mg g^{-1}, respectively, and 128.98, 134.04, 125.78, 109.22 and 85.49 kJ kg^{-1}, respectively, at q_e = 6, 12, 18, 24 and 30 mg g^{-1} for that of GAC. Fig. 13 shows the plot of $\Delta H_{st,a}$ versus q_e. It is found that $\Delta H_{st,a}$ values are positive and that $\Delta H_{st,a}$ decreases as the surface loading increases. The positive values of $\Delta H_{st,a}$ confirm the endothermic nature of the adsorption process. The variation in $\Delta H_{st,a}$ with surface loading can be attributed to the possibility of having lateral interactions between adsorbed Pi molecules.

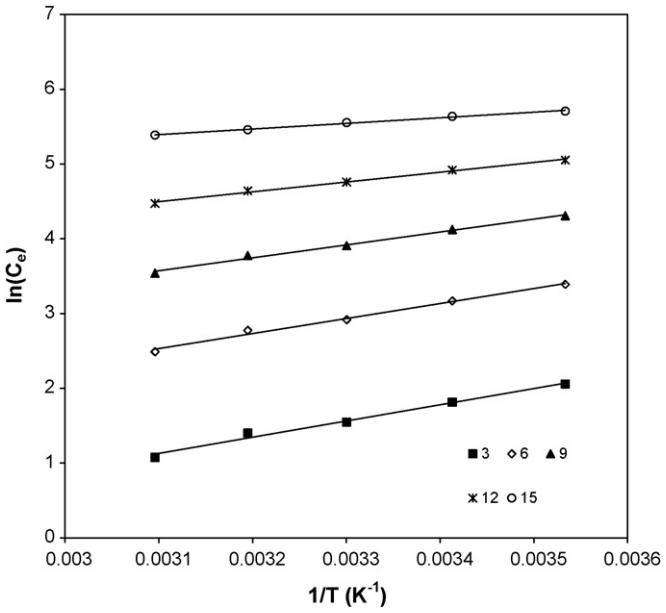

Fig. 11. Isosters to calculate isosteric heat of adsorption for adsorption of Pi onto RHA.

3.8. Desorption of α-picoline

GAC is costlier than RHA, as the RHA is available almost free of cost. Therefore, recovery of Pi and regeneration of GAC after its exhaustion is necessary. The spent RHA may, however, not

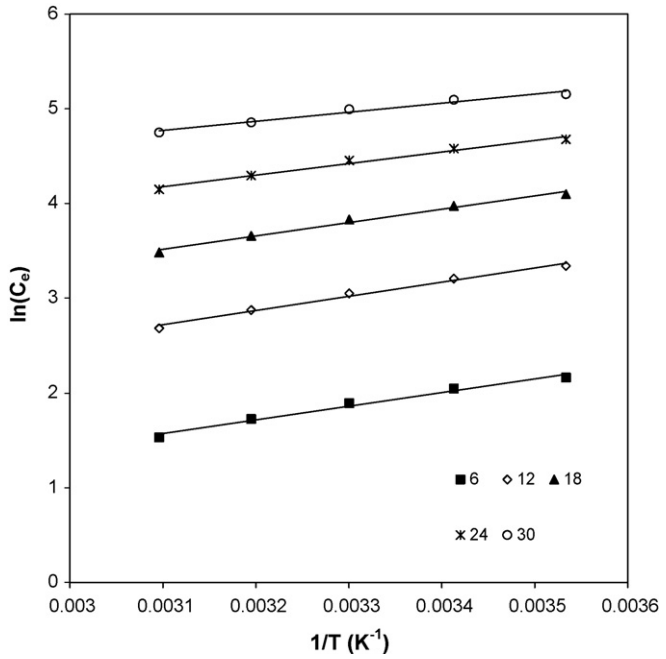

Fig. 12. Isosters to calculate isosteric heat of adsorption for adsorption of Pi onto GAC.

Table 5
Thermodynamic parameters for the adsorption of Pi onto RHA and GAC

Adsorbents	ΔH° (J mol^{-1})	ΔS° (J mol^{-1} K^{-1})	ΔG° (J mol^{-1})				
			283 K	293 K	303 K	313 K	323 K
RHA	20.965	0.127	−15.110	−16.385	−17.660	−18.935	−20.209
GAC	13.898	0.105	−15.923	−16.977	−18.030	−19.084	−20.138

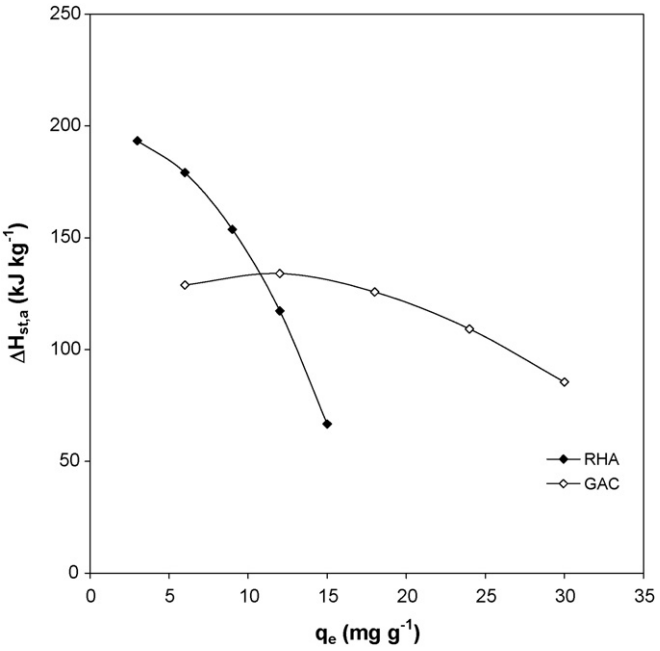

Fig. 13. Variation of isosteric heat of adsorption with surface loading.

be regenerated. Several solvents, viz. DDW (varying pH), 0.1N H_2SO_4, 0.1N HNO_3 and 0.1N NaOH have been used as the eluents to study the characteristics of Pi desorption from GAC and RHA. The desorption experiments were carried out by mixing 1 g Pi loaded adsorbent (RHA: $q_e = 4.74\,mg\,g^{-1}$; GAC: $q_e = 8.82\,mg\,g^{-1}$) with 0.05 dm^3 of the chosen solvent at 303 K and agitated in an orbital shaker for 5 h at 150 rpm. After 5 h, the mixture was centrifuged and the supernatant was analysed for the Pi concentration and the amount of desorbed Pi was determined. Desorption efficiency from RHA was found to be ~72% in water at lower pH, ~85% in H_2SO_4, 70% in HNO_3 and ~7% in NaOH at 303 K. At 288 K temperature, the desorption efficiencies for these solvents were, respectively, 68%, 86%, 78% and 7%. The soil-DDW slurry showed the desorption efficiency of ~3% and ~2% at 303 and 288 K, respectively. It is found that the acidic solutions are able to extract Pi from spent RHA appreciably. For Pi loaded GAC, ~87% Pi was desorbed by water at lower pH. About 89% Pi is desorbed in 0.1N H_2SO_4, ~83% in 0.1N HNO_3 and ~16% in 0.1N NaOH at 303 K and 87%, 89%, 84% and 15% at 288 K, respectively. The soil-distilled water slurry showed the desorption efficiency of about 13 and 9%, respectively, at 303 and 288 K. Thus 0.1N H_2SO_4 can be used to effectively remove Pi from the Pi-loaded GAC for the reuse of GAC. Since the leaching of Pi from RHA and GAC with acidic water is possible, it is necessary to store the spent RHA/GAC safely in containers. After dewatering and drying, the RHA can be fired directly into the furnaces/incinerators to recover its residual energy (~21 MJ kg^{-1}). The spent GAC has to be regenerated and reused. However, the sorption efficiency of GAC is similar to that of RHA and therefore, GAC may not be recommended to be used as an adsorbent for Pi removal from aqueous solution.

3.9. Comparative assessment of RHA and GAC as adsorbent

In order to have the comparative assessment of BFA, RHA, GAC and the ACs manufactured from coconut shells for the sorptive removal of Pi from aqueous solution, it is necessary to compare the C_0/m values of these adsorbents for the comparative C_0 and q_e values. For BFA, the ratio of C_0/m was varied between 10 and 120 mg g^{-1} for the C_0 range of 50–600 mg g^{-1}. The maximum adsorptive uptake, q_e was ~60 mg g^{-1} [5]. Mohan at al. [11] reported the removal of Pi from aqueous solution using SAC and ATSAC. They have used a very low initial Pi concentration (50 mg dm^{-3}), and consequently a low adsorbent dosage (2 g dm^{-3}) with $C_0/m = 25$, for adsorption studies. The q_e values reported by them were ~25 and ~32 mg g^{-1} by SAC and ATSAC, respectively. In the present study, the ratio of C_0/m was varied between 2.5 and 30 mg g^{-1} for RHA, and 5 and 60 mg g^{-1} for that of GAC for the C_0 range of 50–600 mg dm^{-3}. The maximum adsorption uptake, q_e was ~15.46 and 36 mg g^{-1}, respectively by RHA and GAC which is about 25% and 60% of that by BFA [5]. The sorption by RHA and GAC is very fast in comparison to that by SAC and ATSAC. The ultimate removal of Pi in first one h time reported by Mohan et al. [10] is 40–50% and the equilibrium time is 48 h for C_0 of 50 mg dm^{-3}. Whereas, in our earlier study [5] the maximum removal is ~95% and the equilibrium time reported is 6 h for the adsorption of Pi onto BFA for $C_0 = 100$ mg dm^{-3}. In the present study the maximum removal in the first one h is ~90% and ~85% by RHA and GAC, respectively, for $C_0 = 100$ mg dm^{-3} and the equilibrium time is 5 h. Thus, the RHA and GAC are superior to SAC and ATSAC in the Pi sorption rate as well as Pi removal. Mohan et al. [11] have not reported on the desorption of Pi from activated carbons and the regeneration of ACs. The activated carbons are quite costly and, therefore, their regeneration and reuse will be necessary in the sorption process. In contrast, the RHA is available at a throw-away price and hence can be disposed off as a fuel in the boiler furnaces/incinerators after its use in the sorption of Pi. Thus, the RHA becomes a very attractive adsorbent and it can also be used as an alternative to BFA for the removal of Pi from aqueous solutions, even at very high Pi concentrations.

4. Conclusions

The following conclusions can be drawn from the present study:

- The RHA and GAC are good adsorbents for the removal of Pi from aqueous solutions.
- Adsorption rate is found to be very fast. For $C_0 = 100$ mg dm^{-3}, ~90% and ~85% Pi removal in $t = 60$ min contact time at $m = 20$ g dm^{-3} for RHA and 10 g dm^{-3} for GAC, respectively.
- The adsorption of Pi is found to be maximum in the pH_0 range of 6-8 (optimum pH_0 ~6.5).
- The optimum adsorbent dose (m) is found to be 20 and 10 g dm^{-3}, respectively, for RHA and GAC. The maximum uptake of Pi is observed to be 2.34 and 4.55 mg g^{-1} at lower concentration (50 mg dm^{-3}) and 15.46 and 36 mg g^{-1} at higher concentration (600 mg dm^{-3}) at 303 K.
- The lower value of Chi-square error function for any isotherm indicates its adequacy and sufficiency for predicting isotherm data. The Chi-square values were found to be in the order of: Radke–Prausnitz < Toth < Redlich–Peterson < Freundlich < Temkin < Langmuir for Pi adsorption onto RHA; whereas, in the order of Radke–Prausnitz < Redlich–Peterson < Toth < Freundlich < Langmuir < Temkin for the adsorption of Pi onto GAC.
- Thermodynamic analysis and the positive values of isosteric heat of adsorption ($\Delta H_{st,a}$) indicate that the adsorption process is feasible, spontaneous and endothermic in nature. $\Delta H_{st,a}$ varies with the surface loading.
- The uptake of Pi onto GAC is more than that onto RHA owing to the greater surface area of GAC.
- The acidic water can be used as the eluent to regenerate spent adsorbents. However, it is suggested that the spent RHA need not be regenerated and can be used as a fuel and fired in a furnace to recover its energy value and dispose off the Pi-loaded spent RHA.

Acknowledgements

The financial assistance provided by the Ministry of Human Resources Development (MHRD), Govt. of India and the Indian Institute of Technology (IIT), Roorkee to Mr. Dilip H. Lataye is gratefully acknowledged Dr. Lataye also thanks Visvesvaraya National Institute of Technology, Nagpur (India) for allowing him to pursue his Ph.D. work under QIP at IIT Roorkee.

References

[1] F.S. Yates, Pyridine and their benzo derivatives. VI. Applications, in: A.R. Katritzky, C.W. Rees (Eds.), Comprehensive Heterocyclic Chemistry: The Structure, Reaction, Synthesis and Uses of Heterocyclic compounds, vol. 2, Pergaman Press, Oxford, 1984, pp. 511–524 (Part 2A).
[2] K. Othmer, Encyclopedia of Chemical Technology, vol. 15, 3rd ed., John Wiley, New York, 1982, pp. 454–480.
[3] R.J.S.R. Lewis, Sax's Dangerous Properties of Industrial Materials, 11th edition, John Wiley & Sons, New Jersey, 2004, p. 3106.
[4] D.H. Lataye, I.M. Mishra, I.D. Mall, Removal of pyridine from aqueous solution by adsorption on bagasse fly Ash, Ind. Eng. Chem. Res. 45 (11) (2006) 3934–3943.
[5] D.H. Lataye, I.M. Mishra, I.D. Mall, Adsorption of 2-picoline onto bagasse fly ash from aqueous solution, Chem. Eng. J. 138 (2008) 35–46.
[6] G.K. Sims, L.E. Sommers, Biodegradation of pyridine derivatives in soil suspension, Environ. Toxicol. Chem. 5 (1986) 503–510.
[7] V.C. Srivastava, I.D. Mall, I.M. Mishra, Characterization of mesoporous rice husk ash (RHA) and adsorption kinetics of metal ions from aqueous solution onto RHA, J. Hazard. Mater. 134 (1-3) (2006) 257–267.
[8] Q. Feng, Q. Lin, F. Gong, S. Sugita, M. Shoya, Adsorption of lead and mercury by rice husk ash, J. Colloid Interf. Sci. 278 (2004) 1–8.
[9] F. Adam, J.H. Chua, The adsorption of palmytic acid on rice husk ash chemically modified with Al (III) ion using the sol–gel technique, J. Colloid Interf. Sci. 280 (2004) 55–61.
[10] D.H. Lataye, I.M. Mishra, I.D. Mall, Pyridine sorption from aqueous solution by rice husk ash (RHA) and granular activated carbon (GAC): Parametric, kinetic, equilibrium and thermodynamic aspects, J. Hazard. Mater. 154 (2008) 858–870.
[11] D. Mohan, K.P. Singh, S. Sinha, D. Gosh, Removal of pyridine derivatives from aqueous solution by activated carbon developed from agricultural waste materials, Carbon 43 (2005) 1680–1693.
[12] T.L. Gilchrist, Heterocyclic Chemistry, Pitmax Press, London, 1985.
[13] J.B. Weber, Molecular structure and pH effects on the adsorption of 1,3,5-triazine compounds on montmorillonite clay, Am. Miner. 51 (1966) 1657–1690.
[14] S. Zhu, P.R.F. Bell, P.F. Greenfield, Adsorption of pyridine onto spent Rundle oil shale in dilute aqueous solution, Water Res. 22 (10) (1988) 1331–1337.
[15] M.C. Carlos, Adsorption of organic molecules from aqueous solutions on carbon materials, Carbon 42 (2004) 83–94.
[16] L.R. Radovic, C. Moreno-Castilla, J. Rivera-Utrilla, Carbon materials as adsorbents in aqueous solutions, in: L.R. Radovic (Ed.), Chemistry and Physics of Carbon, vol. 27, Marcel Dekker, New York, 2000.
[17] L.R. Radovic, I.F. Silva, J.I. Ume, J.A. Menedez, L.Y. Leon, A.W. Scaroni, An experimental and theoretical study of the adsorption of aromatics possessing electron-withdrawing and electron-donating functional groups by chemically modified activated carbons, Carbon 35 (9) (1997) 1339–1348.
[18] A. Shukla, Y.H. Zhang, P. Dubey, J.L. Margrave, S.S. Shukla, The role of sawdust in the removal of unwanted materials from water, J. Hazard. Mater. B 95 (1/2) (2002) 137–152.
[19] L.J. Yu, S.S. Shukla, K.L. Dorris, A. Shukla, J.L. Margrave, Adsorption of chromium from aqueous solutions by maple sawdust, J. Hazard. Mater. 100 (1–3) (2003) 53–63.
[20] M. Ozacar, I.A. Sengil, Adsorption of metal complex dyes from aqueous solutions by pine sawdust, Bioresource Technol. 96 (7) (2005) 791–795.
[21] I.D. Mall, V.C. Srivastava, N.K. Agarwal, I.M. Mishra, Removal of congo red from aqueous solution by bagasse fly ash and activated carbon: kinetic study and equilibrium isotherm analyses, Chemosphere 61 (2005) 492–501.
[22] S.P. Mishra, V.K. Singh, Radiotracer technique in adsorption study. II. Adsorption of barium and strontium ions on hydrous ceric oxide, Appl. Radiat. Isot. 46 (1995) 75–81.
[23] I. Langmuir, The adsorption of gases on plane surfaces of glass, mica and platinum, J. Am. Chem. Soc. 40 (1918) 1361–1403.
[24] H.M.F. Freundlich, Over the adsorption in solution, J. Phys. Chem. 57 (1906) 385–471.
[25] M.I. Temkin, V. Pyzhev, Kinetics of ammonia synthesis on promoted iron catalysts, Acta. Physiochim. URSS 12 (1940) 327–356.
[26] O. Redlich, D.L. Peterson, A useful adsorption isotherm, J. Phys. Chem. 63 (1959) 1024–1026.
[27] J. Toth, State equations of the solid gas interface layer, Acta Chem. Acad. Hung. 69 (1971) 311–328.
[28] C.J. Radke, J.M. Prausnitz, Thermodynamics of multisolute adsorption from dilute liquid solutions, AIChE J. 18 (1972) 761.
[29] J.M. Smith, H.C. Van Ness, Introduction to Chemical Engineering Thermodynamics, 4th ed., McGraw-Hill, Singapore, 1987.
[30] M. Suzuki, Adsorption Engineering, Kodansha–Elsevier, Tokyo, 1990.
[31] A.A. Khan, R.P. Singh, Adsorption thermodynamics of carbofuran on Sn(IV) arsenosilicate in H^+, Na^+ and Ca^{2+} forms, Colloid Surf. 24 (1987) 33.
[32] V.C. Srivastava, I.D. Mall, I.M. Mishra, Adsorption thermodynamics and isosteric heat of adsorption of toxic metal ions onto bagasse fly ash (BFA) and rice husk ash (RHA), Chem. Eng. J. 132 (1–3) (2007) 267–278.
[33] D.M. Yong, A.D. Crowell, Physical Adsorption of Gases, Butterworths, London, 1962.